1 **Two-Dimensional Versus Three-Dimensional Morphometry of Monogenoidean**

2 **Sclerites**

3 **Paolo Galli[*]; Giovanni Strona[*]; Anna Maria Villa[*]; Francesca Benzoni[*]; Fabrizio Stefani [*];**

4 **Doglia Silvia[*]; and Delane C. Kritsky[†]**

5 [*]Department of Biotechnology and Biosciences, University of Milano-Bicocca, Piazza della Scienza

6 2, 20126 Milano, Italy. *e-mail: paolo.galli@unimib.it*; [†]Department of Health and Nutrition

7 Sciences, Campus Box 8090, Idaho State University, Pocatello, Idaho 83209. *e-mail:*

8 *kritdela@isu.edu*

9

10

11

12

13

14

15

16 Corresponding author:

17 Paolo Galli
18 Dept. of Biotechnology & Biosciences
19 University of Milano-Bicocca
20 Piazza della Scienza 2
21 20126 MILANO
22 e-mail paolo.galli@unimib.it
23 tel. ++39.02.6448.3417
24 fax ++39.02.6448.3450

1

25 **abstract**

26 A new method of three-dimensional analysis of sclerotized structures of monogenoids was

27 performed by processing z-series images with 3D Doctor. Z-series were obtained from

28 Gomori's trichrome-stained specimens of marine and freshwater monogenoids under laser

29 scanning confocal fluorescence microscopy. Measurements obtained from 3-dimensional

30 images were then compared with those from 2-dimensional images taken from both flattened

31 and unflattened specimens. Data comparison demonstrated that 3-dimensional morphometry

32 allows avoidance of over-estimation due to deformation and the reduction of errors associated

33 with different spatial orientations. Moreover, study of 3-dimensional images permits

34 observation of morphological details that are not detectable in 2-dimensional representations.

35
36
37
38
39

40

41

42

43

44

45

46

47

1. INTRODUCTION

During the past two decades, technology of computer-assisted image analysis has rapidly developed, providing biologists with powerful new tools of investigation. Its broad application in science has led to the development of a wide variety of image-data acquisition, treatment and quantification techniques (Müller, 2002), with morphometry receiving major benefit from the technology. The development of these techniques has allowed scientists the ability to overcome limitations on precision associated with obtaining 2-dimensional measurements of 3-dimensional objects. Two-dimensional measurements are generally obtained from a single plane surface, which for microscopic structures is usually represented by the focal plane of an optical microscope, drawings obtained with use of a *camera lucida*, or a photomicrograph (Minnich, 2003, Roff and Hopcroft, 1986).

Since the 1970's, scanning electron microscopy (SEM) has been broadly applied in biology to morphological studies, but such techniques with limited depths of focus provide a false 3-dimensionality to micrographs and requires destruction of specimens to isolate investigated structures (Justine, 1993; Shinn et al., 1993).

Medicine has contributed most to the rapid development of software dedicated to 3-dimensional reconstruction, i.e., 3D-DOCTOR (Able Software Corporation, Lexington, MA 02420, USA), an advanced 3-dimensional modeling, image processing and measurement software used for magnetic resonance imaging (MRI), CT scan and positron emission tomography (PET) for scientific and industrial imaging applications (Enciso *et al.*, 2003; Styner *et al.*, 1999; Müller, 2002). Recently, laser scanning confocal fluorescence microscopy (LSCFM) has been applied to 3-dimensional reconstruction of fungi, invertebrate animals and mammalian cells (Zill *et al.*, 2000; Ebara *et al.*, 2002; Fritz and Turner, 2001; Koehler *et al.*, 2002; Klaus *et al.*, 2002; Neves *et al*, 2005; Schawaroch *et al*, 2005; Sonnek *et al*, 2005; Dickson and Kolesik, 1999). Galli *et al.* (2006)

75 successfully used LSCFN to obtain 3-dimensional images of the haptoral and male copulatory

76 sclerites of members of the Class Monogenoidea (some authors erroneously refer to this class as the

77 "Monogenea," an order of the class Trematoda) stained in Gomori's trichrome (Humason, 1979).

78 These sclerites are generally less than 50μm long, are essential for taxonomic identification and are

79 usually morphologically described and depicted as 2-dimensional drawings obtained by using a

80 *camera lucida* and light microscope. Measurements are usually determined directly from specimens

81 using a microscope equipped with an ocular or filar micrometer, from drawings, or less frequently,

82 using a digitising system on photomicrographs (Ergens, 1969; Chisholm *et al.*, 2001; Davidova *et*

83 *al.*, 2005). The problem with these methods rests with the fact that the sclerites of monogenoids do

84 not normally lie within the visual plane of the microscope, thus requiring that specimens be exposed

85 to moderate to heavy compression on the microscope slide to orient structures to the optical plane of

86 the microscope prior to study (see methods introduced by Malmberg, 1957; Ergens, 1969; Kritsky

87 *et al.*, 1978). Compression always results in the specimen being somewhat damaged or completely

88 destroyed (squashed), inevitably producing both morphologic artefact and metrical error. Moreover,

89 such manipulations irreversibly compromise the natural relative and absolute positions of sclerites

90 in the body, adding to morphometric error during analysis.

91 The purposes of this paper are three fold: 1) to illustrate how z-series images of

92 monogenoidean sclerites obtained from LSCFM can be processed with a 3-dimensional

93 reconstruction and quantification software (3D-Doctor); 2) to compare morphometric results

94 obtained from 3-dimensional morphometric analysis using LSCFM with those collected by

95 traditional methods; and 3) to demonstrate how movies obtained from LSCFM analysis can

96 integrate with original hand drawings of some intricately complex sclerites of these helminths.

97

98 **2. MATERIALS AND METHODS**

99   Monogenoids were collected from marine and freshwater fish: *Kuhnia scombri* (Kuhn, 1829) from

100   *Scomber scombrus* Linnaeus, 1758 (a marine fish from the Mediterranean Sea); *Haliotrema*

101   *curvipenis* Paperna, 1972 from *Mulloidichthys vanicolensis* (Valenciennes, 1831) (a marine fish

102   from the Red Sea); and *Dactylogyrus extensus* Mueller and Van Cleave, 1932 from *Cyprinus carpio*

103   Linnaeus, 1758 (a freshwater fish from Northern Italy). Comparison of measurements obtained

104   from 2- and 3-dimensional morphometric analyses were performed using specimens of *D. extensus*,

105   while subjects for LSCFM studies included specimens of all three parasite species.

2.1   Processing specimens for confocal microscopy

107   Gill baskets of respective hosts were removed at the site of collection and placed in containers of

108   hot (60° C) 4-5% formalin to relax and fix the attached monogenoids. Fixed gills were placed in

109   vials containing the respective fluid, labeled and stored until study. A formalin-fixed specimen(s)

110   was subsequently removed from the gills or picked from the sediment using a fine probe and

111   dissecting microscope and placed in 1 Normal NaOH for 10 min before being transferred to a small

112   droplet of Gomori's trichrome (Humason, 1979) located near the center of a small disposable Petri

113   dish. After 1-2 minutes, the droplet containing the specimen(s) was flooded with absolute ethanol

114   to cease absorption of stain. Destaining of the specimen(s) was accomplished by adding water to

115   the dish to dilute the ethanol-stain mixture to about 50%. When the desired level of stain remained

116   in the specimen, the helminth was removed with a fine probe and placed in absolute ethanol for

117   about 1 min, after which it was transferred to beachwood creosote for clearing and mounting in

118   euparal.

2.2 Confocal microscopy

120   LSCFM images of monogenoids were obtained by using a Leica TCS SP2 confocal microscope

121   coupled to an inverted Leica DMIRE2 microscope equipped with a PL APO 63x oil immersion

122   objective (N.A. = 1.4). The sample was excited with the argon laser at 515 nm, and fluorescence

123 emission was collected through a band-pass filter between 525 nm and 730 nm. Images (8-bit) with

124 1,024 x 1,024 pixels per frame were obtained. Z-series were collected with a step size of 0.115 μm

125 to maximize axial resolution of 3-dimensional images.

126 *2.3* **Morphometric analysis**

127 For 2- and 3-dimensional morphometric analyses, 10 *D. extensus* were prepared according to the

128 procedures described above, and another 10 specimens of *D. extensus* were collected alive from the

129 gills of *C. carpio* and flattened with coverslips on slides in ammonium picrate glycerine according

130 to the procedures of Malmberg (1957). Eight linear measurements, illustrated in figure 1, were used

131 to compare the methods of morphometric analysis. Specimens prepared under both methods

132 (Gomori's trichrome and ammonium picrate) were observed with an optical microscope equipped

133 with phase contrast and a calibrated micrometric lens to obtain the 2-dimensional measurements of

134 the haptoral and copulatory sclerites. Z-series in TIFF format were then collected from the ten

135 specimens stained with Gomori's trichrome using LSCFM and then loaded onto 3D-Doctor

136 software 4.0.061025 (Able Software Corporation). Voxel were calibrated using the TXT report file

137 automatically generated by LCS. Image contrast and thresholds for segmentation were manually

138 calibrated in order to maximize resolution and minimize loss of digital information. Three-

139 dimensional surface models of each structure of interest were generated, and linear measurements

140 were obtained with the dedicated tool in 3D-Doctor after appropriate rotation of the 3-dimensional

141 objects. A Principal Components Analysis (PCA) was conducted on data collected using the three

142 methods in order to determine possible multivariate distinctions. A Fisher's f test with an 95%

143 confidence interval was performed on the morphometric data to evaluate comparability among the

144 three methods of measurement. Finally, considering Fishers' f test results, a 95% Student's t test

145 was applied to the same data, to verify affects of the measuring procedures on mean values.

146 *2.4* **Morphological analysis**

147 From the 3-dimensional reconstructions of sclerites that were developed from the z-series using

148 both the Leica LCS software and 3D-Doctor software, movies were produced and exported in AVI

149 or WMV format. Interactive observation of 3-dimensional models rotated along axes enabled

150 choice of orientations from animations in order to observe and study hidden or complex details of

151 the respective sclerites. Transparency filters were applied when necessary.

152

3. RESULTS

3.1 Morphometric analysis

155 Linear parameters obtained from 3-dimensional reconstructions and 2-dimensional preparations

156 (flattened and unflattened specimens) of the haptoral and copulatory sclerites of *D. extensus* are

157 presented in figure 1. For all parameters, mean measurements obtained from the 3-dimensional

158 reconstructions fell between those obtained from specimens prepared for 2-dimensional

159 observations, with those from unflattened specimens being smaller and those of flattened specimens

160 being larger than the respective 3-dimensional parameters; the majority of the respective

161 measurements from the different preparations is significantly different (P = 0.05) (Table 1).

162 Variation within means obtained from LSCFM preparations and flattened specimens were

163 comparable (Fig. 2); a scores' plot of the Principal Component Analysis is shown in Fig. 3, where

164 greatest variation among individual mean measurements from the respective preparations was also

165 observed among those obtained from unflattened specimens.

3.2 Morphological analysis

167 Specimens stained with Gomori's trichrome and mounted in euparal show fluorescence of all

168 haptoral and copulatory sclerites when excited at 515 nm by argon laser. Fluorescence was highly

169 stable and localized on the surface of sclerites, both of which are important because hundreds of z-

170   section images are usually required for high-resolution 3-dimensional reconstructions of these

171   comparatively thick sclerotized structures.

172   A modified drawing of the figure of the copulatory complex of *Haliotrema curvipenis*

173   presented by Paperna (1972) in the original description of the species and a 3-dimensional LSCFM

174   reconstruction are shown in Figs. 4a and 4b, respectively; movie 1 shows the 3-dimensional

175   reconstruction of the copulatory complex rotated through approximately 360°. While the original

176   drawing of the copulatory complex is a reasonable representation, the 3-dimensional reconstruction

177   shows considerably more detail of the relationships of the complex base, proximal orifice and shaft

178   of the copulatory organ. An accessory piece is absent, and the base of the copulatory organ serves

179   as a guide for the copulatory shaft; the proximal portion of the copulatory shaft is dorsoventrally

180   compressed, and the distal portion is laterally compressed. Similarly, details of the dorsal and

181   ventral anchor/bar complexes of *H. curvipenis* are greatly enhanced using LSCFM reconstructions

182   (dorsal and ventral bars and anchors are respectively shown in Fig. 5 (b-c) and Movie 2).

183   In Fig. 6 and Movie 3, depictions of genital corona of *Kuhnia scombri* obtained from 2-

184   dimensional methods (modified from Sproston, 1945 ~~modified~~) and a LSCFM reconstruction are

185   compared. In these comparisons, like those of *H. curvipenis*, the morphological details and

186   relationships of the component parts of each of these structures are greatly enhanced using 3-

187   dimensional reconstructions over 2-dimensional hand representations.

188

189   **4. DISCUSSION**

190   *4.1* **Morphometric analysis**

191   While compression of specimens may limit variation in measurements by eliminating error due to

192   spatial orientation, flattening of specimens can lead to over-estimation of size due to structural

193   distortion. Such error becomes more evident for small, more delicate, distortable and deformable

194 structures. Similarly, 2-dimensional measurements performed on unflattened specimens may avoid

195 distortion and deformation, but these measurements generally represent underestimations resulting

196 from non-planar orientations of structures. Three-dimensional measurements, however, are not

197 affected by either of these problems as acquisition of the third dimension eliminates problems

198 associated with spatial orientation and distortion.

199 Such observations, supported by results obtained during the present study, agree with those

200 of Minnich (2000). In the majority of linear measurements (Fig. 2), means and standard deviations

201 from 3-dimensional measurements fell between 2-dimensional measurements taken on unflattened

202 and flattened specimens, respectively. Among the three methods, maximum means for the eight

203 dimensions were always observed in 2-dimensional measurements of compressed specimens, while

204 maximum ranges were detected in 87.5% of cases of 2-dimensional measurements of unflattened

205 specimens.

206 Principal Component Analysis indicates that data obtained by the three methods of

207 measurememt group into separate clusters (Figure 3). The first two components are significant and

208 represent 69.0% of the total variance. Student's t test (Table 1) indicates that mean values of

209 dimensions A, B, C, D, and F obtained from 3-dimensional and 2-dimensional (unflattened) images

210 of the anchors, bar and copulatory apparatus do not differ significantly, although the Fisher's f test

211 (Table 1) suggests significant differences in variances for the same parameters. This inconsistency

212 is apparently attributed to small differences in rotation around the main axis of structures and to

213 results reflecting accuracy more than precision during the measuring process. Comparison between

214 flattened (2D) and unflattened (2D and 3D) measurements indicates that differences, linked to

215 deformation and distortion from specimen compression, are statistically significant in 84% of cases

216 for both t- and f-tests, confirming the results obtained by Justine (2005), who showed that as much

217   as 20% deformation (p<0.001) results in the internal soft organs of the body and in the haptoral and

218   copulatory sclerities of monogenoids when specimens are compressed.

219   *4.2 Morphological analysis*

220   In this paper, LSCFM of monogenoids stained with Gomori's trichrome was shown to allow

221   reconstruction of 3-dimensional images of sclerites while avoiding artefacts resulting from

222   distortion, elongation, rupture or shifting of sclerites from original positions due to specimen

223   compression. For example in Paperna's (1972) hand drawings of haptoral structures of *Haliotrema*

224   *curvipenis*, the ventral bar appears to occur in two pieces, while LSCFM images clearly show that

225   the two ends of the bar are connected by a thin medial constriction (Fig. 5). Moreover, the

226   anteroposterior and dorsoventral views of both ventral and dorsal bars of *H. curvipenis* show higher

227   degrees of complexity than that suggested by Paperna's original drawings (Fig. 5). Although

228   morphologically comparable with Paperna's *camera lucida* drawing of the male copulatory organ of

229   *H. curvipenis,* 3-dimensional images indicate that an accessory piece is absent in this species (Fig.

230   4, Movie 1).

231   Movie 4 provides an animation of the 3-dimensional reconstruction of a clamp of *Kuhnia*

232   *scombri*. The movie highlights the two distinct parts of the midsclerite of the clamp (an anterior

233   discoid and a posterior oval portion), for which Sproston (1945) required 6 different drawings to

234   fully render and describe the structure as a single piece. Because Gomori's trichrome is commonly

235   used to stain soft organs of monogenoids for light microscopic study, researchers may now use the

236   same specimens to also observe the sclerites of these helminths using LSCFM without destruction

237   or damage to the specimen. Three-dimensional reconstructions allow observation of unique details

238   of sclerites generally not observable with light transmission microscopy. For example, the true

239   shape and position of the different parts of the genital corona of *Kuhnia scombri* are only visible

240   using LSCFM (Fig. 6) as shown by the two major spines of the genital corona being more laterally

241   located and not anterolaterally as originally depicted by Sproston (1945). Further, the morphology

242   of the genital corona and the orientation of its spines can be better appreciated in Movie 3, where

243   ten spines with inwardly oriented points are observed in the central corona, while the 2 lateral

244   spines have outwardly oriented points. When flattened specimens were used as in the case of

245   Sproston's data, it is difficult to establish whether the observed variability in the number of coronal

246   spines in *K. scombri* was normal or due to sample preparation. Because LSCFM does not require

247   mechanical action on the specimen, it was possible to assess whether or not differences in the

248   number of spines (11 to 13 among 5 examined specimens) was attributable to intrinsic variability or

249   are artefacts introduced during specimen preparation

250   The quality of the morphological detail of structures and the relative ease of development of

251   the movies (about 20 min to stain and fix a specimen on a slide and 1 hr for LSCFM analysis) allow

252   rapid acquisition of information not achievable with traditional methods using light transmission

253   microscopy. Because many reference and type specimens of monogenoids deposited in museums

254   are stained with Gomori's trichrome, it is now possible to review this material with LSCFM in

255   order to obtain additional morphological information without damage to respective specimens. It

256   would also be possible to integrate museum collections of monogenoids with a database of 3-

257   dimensional images of haptoral and copulatory sclerites for further reference.

258 **REFERENCES**

259 Chisholm, L., Whittington, I. D., Kearn, G. C., 2001. *Dendromonocotyle colorni* sp.n. (Monogenea:

260 Monocotytlidae) from the skin of *Himantura uarnak* (Dasyatididae) from Israel and a new host

261 record for *D. octodiscus* from the Bahamas. *Folia Parasitol.* 48: 15-20.

262 Davidova, M., Jarkovsky´, J., Matějusovà, I., Gelnar, M., 2005. Seasonal occurrence and metrical

263 variability of *Gyrodactylus rhodei Zˇitnˇan* 1964 (Monogenea, Gyrodactylidae), *Parasitol. Res.* 95:

264 398–405.

265 Dickson S. and Kolesik P., 1999. Visualisation of mycorrhizal fungal structures and quantification

266 of their surface area and volume using laser scanning confocal microscopy. *Mycorrhiza*. 9: 205-213.

267 Ebara S., Kumamoto K., Matsuura T., Mazurkiewicz J. E., Rice F. L., 2002 Similarities and

268 differences in the innervation of mystacial vibrissal follicle-sinus complexes in the rat and cat: a

269 confocal microscopic study. *J. Comp. Neurol..* 449(2):103-19, 2002 Jul 22.

270 Enciso, R., Memon, A., Mah, J., 2003. Three-dimensional visualization of the craniofacial patient:

271 volume segmentation, data integration and animation *Orthod. Craniofacial Res*. 6: 66–71.

272 Ergens, R., 1969. The suitability of ammonium picrate-glycerin in preparing slides of lower

273 Monogenoidea. *Folia Parasitol.* 16: 320.

274 Fritz, A. H., Turner, F. R., 2001. A light and electron microscopical study of the spermathecae and

275 ventral receptacle of Anastrepha suspensa (Diptera: Tephritidae) and implications in female

276 influence of sperm storage. *Arthropod Structure and Development*. Elsevier Science Ltd, Oxford,

277 UK: 2001. 30: 4, 293-313.

278 Galli P., Strona G., Villa A. M, Benzoni F., Stefani F., Doglia S. M., Kritsky D., 2006. Three-

279 Dimensional Imaging of Monogenoidean Sclerites By Confocal Laser Scanning Microscopy. *J.*

280 *Parasitol.* 92: 2, 395-399.

281 Humason G.L., 1979: Animal Tissue Techniques. W.H. Freeman Co., San Francisco, USA, 661 pp.

282 Justine, J.L., 1993. Ultrastructure des monogènes: listes des espèces et des organes étudié. Bull.

283 Fr. Peche Piscic. 328: 156-188

284 Justine J. L., 2005. Species of *Pseudorhabdosynochus* Yamaguti, 1958 (Monogenea: Diplectanidae)

285 from *Epinephelus fasciatus* and *E. merra* (Perciformes: Serranidae) off New Caledonia and other

286 parts of the Indo-Pacific Ocean, with a comparison of measurements of specimens prepared using

287 different methods, and a description of *P. caledonicus* n. sp. *Syst. Parasitol*. 62: 1-37

288 Klaus A. V., Kulasekera V. L., Schawaroch V., 2002. Three-dimensional visualization of insect

289 morphology using confocal laser scanning microscopy. *J. Microsc.* 212: 107-121.

290 Koehler A., Zia C., Desser S.S., 2002 Structural organization of the midgut musculature in black

291 flies (*Simulium* spp.). *Can. J. Zoolog.* 80 (5): 910-917.

292 Kritsky, D.C., Leiby, P.D., Kayton, R.J., 1978. A rapid stain technique for the haptoral bars of

293 *Gyrodactylus* species (Monogenea). *J. Parasitol.,* 64(1), 172-174

294 Malmberg, G., 1957. Om förekomsten av *Gyrodactylus* på svenska fiskar. *Särtryck ur Skrifter*

295 *utgivna av Södra Sveriges Fiskeriförening, Årsskrift* 1956, 19-76

296 Minnich, B., Lametschwandtner, A., 2000. Lengths measurements in microvascular corrosion

297 castings: two-dimensional versus three-dimensional morphometry. *Scanning*, 22(3):173-7)

298 Minnich, B., Krautgartner W-D., Lametschwandtner, A., 2003. Quantitative 3D Analysis in SEM:

299 A Review. *Microsc. Microanal.,*9: 118.

300 Müller, R., 2002. The Zürich Experience: One Decade of Three-Dimensional High-Resolution

301 Computed Tomography. *Top. Magn. Reson. Imag.*, 13(5): 307–322.

302 Neves R. H., Biolchini, C. de L., Machado-Silva, J. R., Carvalho, J. J., Branquinho, T. B., Lenzi, H.

303 L., Hulstijn, M., Gomes, D. C., 2005. A new descriptioin of the reproductive system of

304 *Schistosoma mansoni* (Trematoda: Schistosomatidae) analyzed by confocal laser scanning

305 microscopy. *Parasitol. Res.* 95: 43-49.

306 Paperna, I., 1972. Monogenea from Red Sea fishes. II Monogenea of Mullidae. *P. Helm. Soc.*

307 *Wash.* 39: 39-45.

308 Roff J.C., Hopcroft R.R., 1986. High precision microcomputer based measuring system for

309 ecological research. *Can. J. Fish Aquat. Sci.*, 43:2044-2048.

310   Schawaroch, V., Grimaldi, D., Klaus A. V., 2005. Focusing on morphology: applications and

311   implications of confocal laser scanning microscopy (Diptera: Campichoetaetidae, Camillidae, and

312   Drosophilidae). *P. Helm. Soc. Wash*. 107: 323-335.

313   Shinn A.P. Gibson D.I., Sommerville C., 1993. An SEM study of the haptoral sclerites of the genus

314   *Gyrodactylus* Nordmann, 1832 (Monogenea) following extraction by digestion and sonication

315   techniques. Systematic Parasitology 25: 135–144.

316   Sonnek R., Zurawski H., Gelnar M., 2005. Gross anatomy of the muscle system of *Eudiplozoon*

317   *nipponicum* as visualised by confocal Microscopy. *5th International Symposium on Monogenea*.

318   Guangzhou, China August 8 -12. 2005.

319   Sproston, N. G., 1945. The genus *Kuhnia* n. g. (Trematoda: Monogenea). An examination of the

320   value of some specific characters, including factors of relative growth. *Parasitology*. 36: 176-90.

321   Styner, M., Coradi, T., Gerig, G., 1999. Brain morphometry by distance measurement in a non-

322   Euclidean, curvilinear space. *In 1999 proceedings of Image Processing in Medical Imaging* (IPMI),

323   LNCS 1613: 364-369.

324   Zill S., Frazier S. F., Neff D., Quimby L., Carney M., Di Caprio R., Thuma J., Norton M., 2000.

325   Three-dimensional graphic reconstruction of the insect exoskeleton through confocal imaging of

326   endogenous fluorescence. *Microsc. Res. Techniq*. 48: 367-384.

FIGURES AND TABLE LEGENDS

Figure 1- Three dimensional reconstruction of haptoral and copulatory structures of *Dactylogyrus extensus* Mueller and Van Cleave, 1932, with indication of considered linear measurements. I: Anchor (A, superficial root edge to point tip; B, shaft edge to point tip; C, deep root edge to point tip); II: Bar (D, bar length; E, bar width); III: Male copulatory organ with accessory piece (F, length; G, width); IV: Hook (H, hook length).

Figure 2- Box plots summarizing descriptive statistics of 3D and 2D (both on flattened and unflattened specimens) measurements of haptoral and copulatory sclerites of *Dactylogyrus extensus* Mueller and Van Cleave, 1932. Capital letters refer to Figure 1, and for each corresponding triad the box plots represents respectively (left to right): first, 2D measurements on unflattened specimens; second, 3D measurements; third 2D measurements on flattened specimens. ▬ : average values; ● : minimum and maximum values. Number of observations: A, B and C =20; D, E, F and G =10; H = 50.

Figure 3 – Scores' plot of the PCA, with respect to the first two components, representing 69% of the total variance; ●: 2D Flattened Measurements; ▲: 3D Measurements; ■: 2D Unflattened Measurements.

Figure 4 - a: copulatory organ of *Halitrema curvipenis* drawing with *camera lucida* (Paperna, 1972 modified); b: three views of the same structure realised using Laser Scanning Confocal Fluorescence Microscopy.

350   Figure 5 – a: hooks and bars of *Haliotrema curvipenis* drowing with *camera lucida* (Paperna, 1972

351   modified); b: ventral bar of *H. curvipenis* realised using LSCFM image (i: anteroposterior view; ii:

352   dorsoventral view); c: dorsal bar of *H. curvipenis* realised using laser scanning confocal

353   fluorescence microscopy image (i:anteroposterior view; ii: dorsoventral view).

354

355   Figure 6- a: hand drawing of genital atrium of *Kuhnia scombri* (Sproston, 1945 modified); b-d:

356   various views of LSCFM image.

357

358   Table 1 – Pairwise statistical comparisons of the data sets acquired with three different measuring

359   methods . The comparisons have been tested by means of Fisher's F test (F test, $p < 0.05$) and

360   Student's t test (t test, $p < 0.05$).

361   A-H: linear measurements of haptoral and copulatory sclerites of *Dactylogyrus extensus*, as shown in

362   fig.1. * significantly different comparisons.

Figure 1

Figure 2
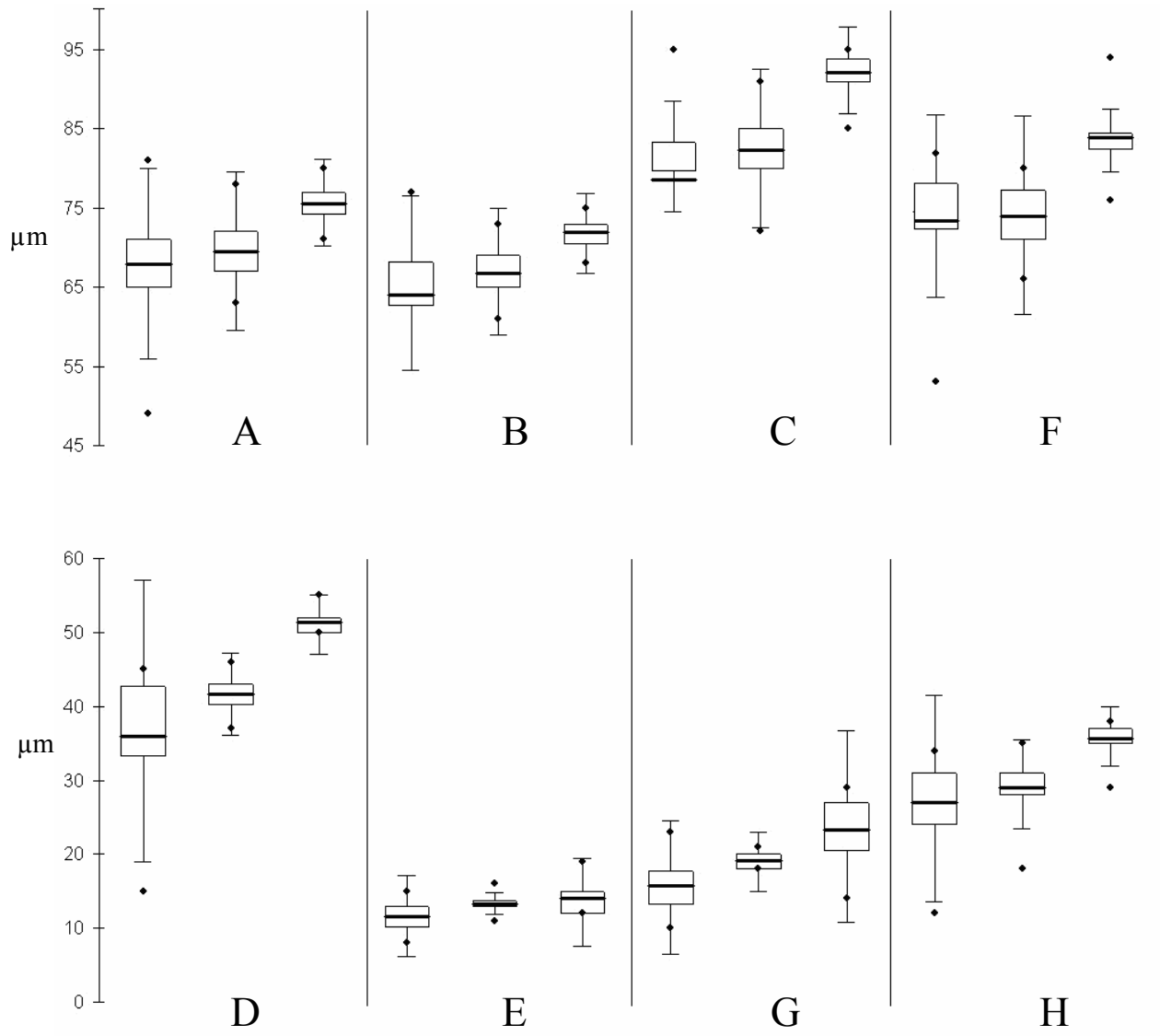
Figure 3

3D V.S. 2D FLATTENED V.S. 2D UNFLATTENED
Observations on axes 1 and 2 (69%)
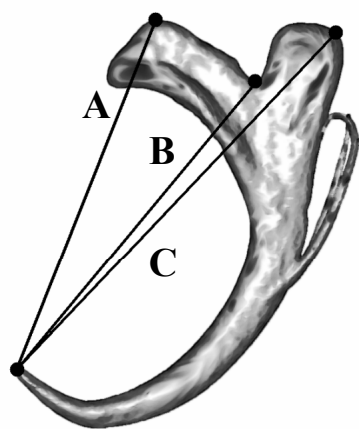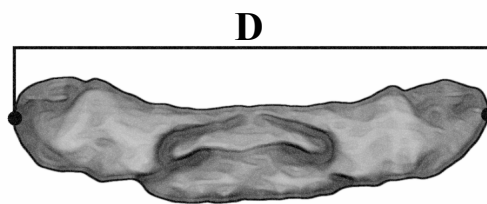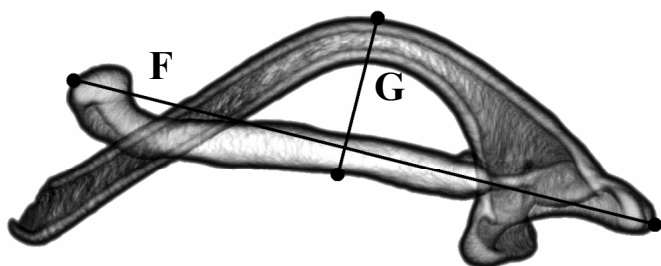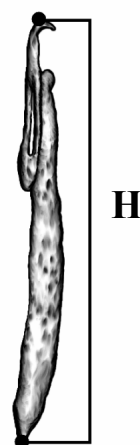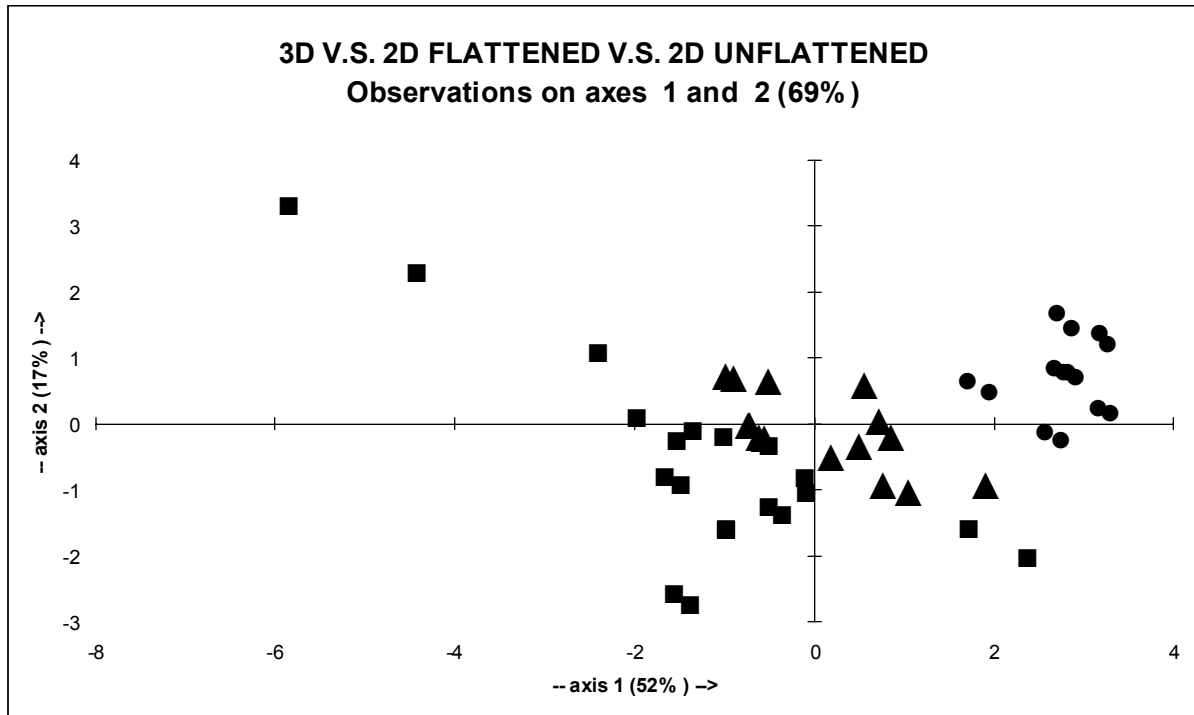
Figure 4

a   b

Figure 5

a

b i

b ii

c i

c ii
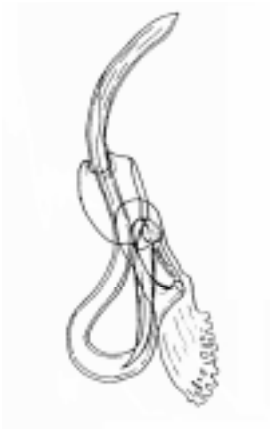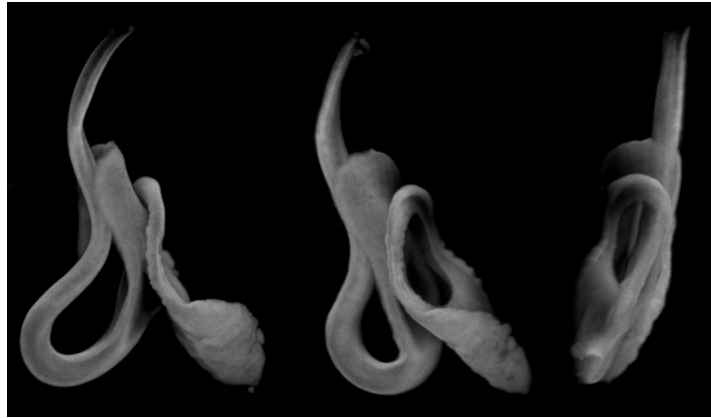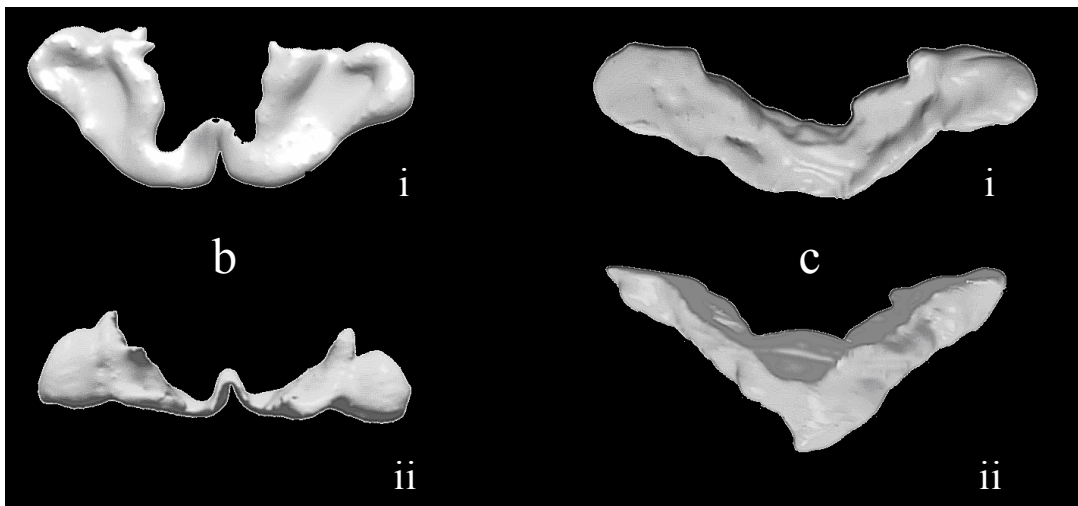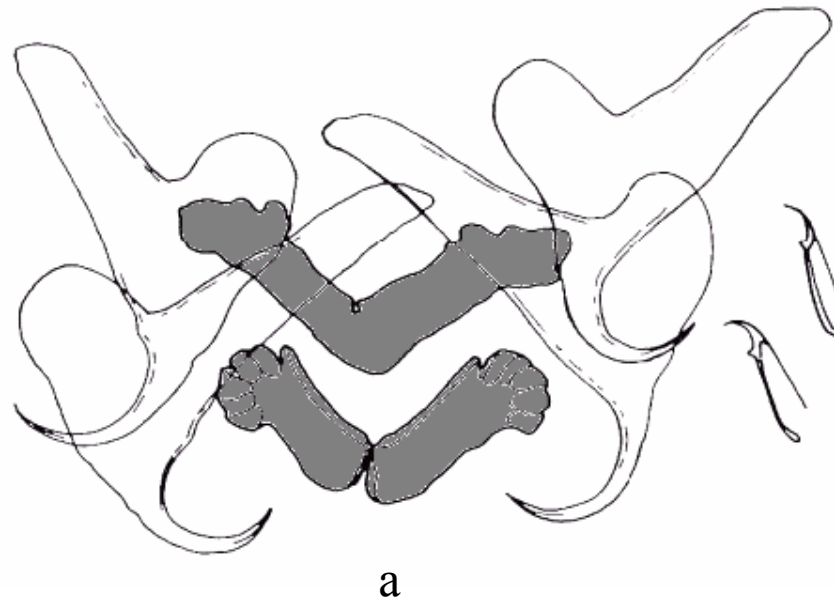
Figure 6
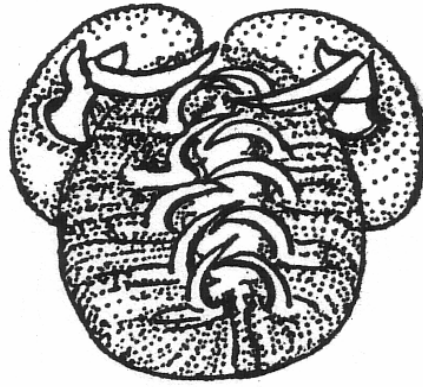
a
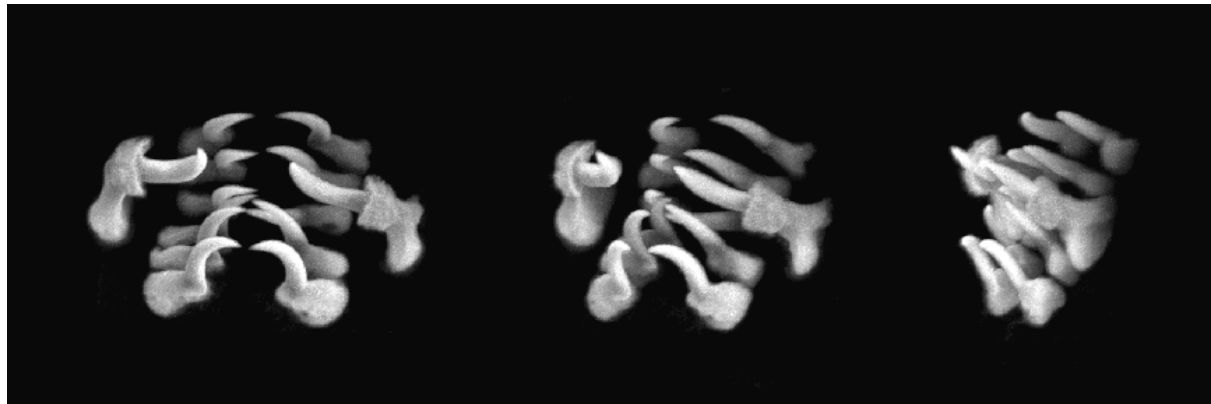
b   c   d

Table 1

		A	B	C	D	E	F	G	H
3D Measurements V.S. 2D Unflattened	F test	3.67*	9.79*	7.35*	11.98*	3.09*	4.15*	15.59*	2.44
	t test	-0.78*	-1.17*	-1.28*	-1.31*	-2.23°	-0.02*	-3.28°	-3.08°
2D Unflattened V.S. 2D Flattened	F test	12.49*	23.34*	24.68*	34.46*	1.01	3.70*	1.30	16.60*
	t test	-3.37°	-3.05°	-4.12°	-4.95°	-2.51°	-3.36°	-4.54°	-12.88°
3D Measurements V.S. 2D Flattened	F test	3.40*	2.38	3.36*	2.88*	3.11*	1.12	20.25*	6.81*
	t test	-4.43°	-4.97°	-6.75°	-10.91°	-0.86*	-5.27°	-3.00°	-13.99°

movie 1
Click here to download Multi-media supplement: movie 1.WMV

movie 2
Click here to download Multi-media supplement: movie 2.WMV

movie 2
Click here to download Multi-media supplement: movie 2.WMV

movie 3

[Click here to download Multi-media supplement: movie 3.WMV](#)

movie 4

Click here to download Multi-media supplement: movie 4.wmv

movie 4

Click here to download Multi-media supplement: movie 4.wmv